

# THEORETICAL DYNAMICS ANALYSIS OF THE MOLTEN-SALT REACTOR EXPERIMENT

REACTORS

T. W. KERLIN, S. J. BALL, and R. C. STEFFY\*  
Oak Ridge National Laboratory, Oak Ridge, Tennessee 37830

**KEYWORDS:** reactors, reactivity, uranium-233, uranium-235, transients, disturbances, frequency, variations, stability, fuels, operation, differential equations, MSRE, reactor kinetics

Received May 23, 1970  
Revised September 14, 1970

*The dynamic characteristics of the MSRE were calculated for operation with  $^{235}\text{U}$  and  $^{233}\text{U}$  fuels. The analysis included calculation of the transient response for reactivity perturbations, frequency response for reactivity perturbations, stability, and sensitivity to parameter variations. The calculations showed that the system dynamic behavior is satisfactory for both fuel loadings.*

## I. INTRODUCTION

The dynamic characteristics of the Molten-Salt Reactor Experiment (MSRE) were studied carefully prior to the initial  $^{235}\text{U}$  fuel loading in 1965 and again prior to the  $^{233}\text{U}$  fuel loading in 1968. The first objective of these studies was to determine the safety and operability of the system. The second objective was to establish methods of analysis which can be used with confidence in predicting the dynamic behavior of future, high-performance molten-salt reactors. To satisfy the second objective, it was necessary to include theoretical predictions of quantities amenable to experimental measurement. The frequency response results proved most useful for this purpose.<sup>1</sup>

Several different types of calculations were used in these studies. In general, they consisted of calculations of transient response, frequency response, stability, and parameter sensitivities. Four considerations led to the decision to use this many different types of analysis. These were:

1. It is helpful to display system dynamic characteristics from different points of view as an aid in understanding the underlying physical causes for calculated behavior.

2. Computer costs for the different types of analysis were small compared to the expense of preparing the mathematical models.

3. The calculations for comparison with experiment (frequency response) were essential, but they did not furnish sufficient information about the system.

4. The experience with a number of methods provided insight on selecting methods which would be most useful in analysis of future molten-salt reactors.

The analysis of the system with  $^{233}\text{U}$  fuel was very similar to the analysis of the  $^{235}\text{U}$ -fueled system. The modeling for the  $^{233}\text{U}$  study was influenced slightly by results from dynamics experiments on the  $^{235}\text{U}$ -fueled system and the analysis for the  $^{233}\text{U}$ -fueled system took advantage of some new methods developed after the completion of the first study.

This paper describes the mathematical models used, the computational methods used, and the results of the calculations. A companion paper<sup>1</sup> gives results of dynamics experiments and comparisons with theoretical predictions.

## II. DESCRIPTION OF THE MSRE

The MSRE is a graphite-moderated, circulating-fuel reactor with fluoride salts of uranium, lithium, beryllium, and zirconium as the fuel.<sup>2</sup> The basic flow diagram is shown in Fig. 1. The

\*Present address: Tennessee Valley Authority, Chattanooga, Tennessee.

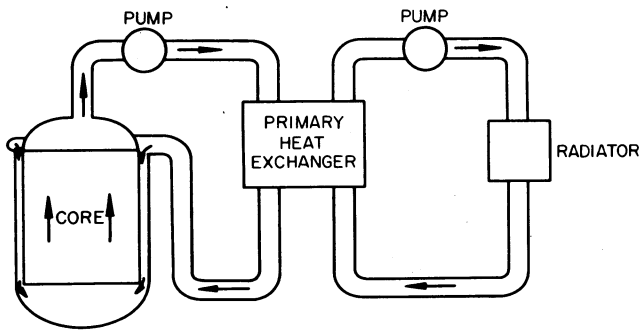


Fig. 1. MSRE basic flow diagram.

molten, fuel-bearing salt enters the core matrix at the bottom and passes up through the core in channels machined out of 2-in. graphite blocks. The 8 MW of heat generated in the fuel and transferred from the graphite raises the fuel temperature from 1170°F at the inlet to 1210°F at the outlet. When the system operates at low power, the flow rate is the same as at 8 MW, and the temperature rise through the core decreases. The high-temperature fuel salt travels to the primary heat exchanger, where it transfers heat to a non-fueled secondary salt before reentering the core. The heated secondary salt travels to an air-cooled radiator before returning to the primary heat exchanger.

Criticality was first achieved with  $^{235}\text{U}$  fuel (35 at. %  $^{235}\text{U}$ ) in June of 1965. After 9006 equivalent full power hours of operation, this uranium was removed and the reactor was refueled with  $^{233}\text{U}$  (91.5 at. %  $^{233}\text{U}$ ) in October of 1968. Between October 1968, and shutdown in December 1969, an additional 4166 equivalent full power hours were achieved with  $^{233}\text{U}$  fuel.

Dynamically, the two most important characteristics of the MSRE are that the core is heterogeneous and that the fuel circulates. Since this combination of important characteristics is uncommon, a detailed study of system dynamics and stability was required. The fuel circulation acts to reduce the effective delayed-neutron fraction, to reduce the rate of fuel temperature change during a power change, and to introduce delayed fuel-temperature and neutron-production effects. The heterogeneity introduces a delayed feedback effect due to graphite temperature changes.

### III. SYSTEM MODELS

#### A. Neutronics

The point kinetics equations for circulating fuel reactors were used with appropriate temperature-

dependent reactivity feedback (see Sec. III.C). The equations are<sup>3</sup>:

$$\frac{d\delta n}{dt} = \left( \frac{\rho_0 - \beta_T}{\Lambda} \right) \delta n + \left( \frac{n_0}{\Lambda} \right) \delta \rho + \sum_{i=1}^6 \lambda_i \delta c_i + \frac{\delta \rho \delta n}{\Lambda} \quad (1)$$

$$\frac{d\delta c_i}{dt} = \frac{\beta_i}{\Lambda} \delta n - \lambda_i \delta c_i - \frac{\delta c_i}{\tau_c} + \frac{\delta c_i(t - \tau_L) \exp(-\lambda_i \tau_L)}{\tau_c}, \quad (2)$$

where

$\delta n$  = deviation in neutron population from steady state

$\delta c_i$  = deviation in concentration of the  $i$ 'th precursor group from steady state

$\rho_0$  = reactivity change in going from a circulating fuel condition to a stationary fuel condition

$\beta_T$  = total delayed-neutron fraction

$\beta_i$  = importance weighted delayed-neutron fraction for the  $i$ 'th precursor group

$\Lambda$  = neutron generation time

$\delta \rho$  = change in reactivity

$\lambda_i$  = radioactive decay constant for the  $i$ 'th precursor group

$\tau_c$  = fuel residence time in the core

$\tau_L$  = fuel residence time in the external loop.

The term  $\delta \rho$  is given by

$$\delta \rho = \delta \rho_r + \sum \alpha_i \delta T_i,$$

where

$\delta \rho_r$  = reactivity change due to control-rod motion

$\alpha_i$  = temperature coefficient of reactivity for the  $i$ 'th section (node) of the core

$\delta T_i$  = temperature change in the  $i$ 'th section (node) of the core.

In some of the calculations (determination of eigenvalues of the system matrix), it was necessary to eliminate the time delay from the precursor equation. This was accomplished by eliminating the last two terms from Eq. (2) and defining an effective  $\beta_i$  as follows:

$$\beta_{i \text{ eff}} = \beta_i \times \left( \frac{\text{delayed neutrons emitted in core at steady state}}{\text{total delayed neutrons emitted in the system at steady state}} \right).$$

Then, the approximate precursor equation is

$$\frac{d\delta c_i}{dt} = \frac{\beta_i^{\text{eff}}}{\Lambda} \delta n - \lambda_i \delta c_i \quad (3)$$

This formulation assumes that the fraction of the precursors which decay in in-core regions is constant during a transient. Comparison of frequency response calculations using this approach and an approach which explicitly treats circulating precursor effects showed negligible differences in the frequency range of interest.

Since the neutron population is proportional to fission power, the units on  $\delta n$  were taken to be megawatts.

### B. Power

An attempt was made to include the effect of delayed gamma rays on the total power generation rate. If we assume that the delayed gamma rays are emitted by a single nuclide, then the appropriate equation is

$$\frac{dN}{dt} = \gamma n - \lambda N \quad (4)$$

where

$N$  = energy stored in gamma-ray emitters (in MW sec)

$\gamma$  = fraction of power which is delayed

$n$  = neutron population (in units of MW)

$\lambda$  = decay constant of gamma-ray emitter ( $\text{sec}^{-1}$ ).

The total power is given by

$$P = \lambda N + (1 - \gamma)n \quad (5)$$

For these studies the value used for  $\lambda$  and  $\gamma$  were 0.0053 and 0.066/sec, respectively.

### C. Core Heat Transfer

The core heat transfer was modeled using a multinode approach. The reactor was subdivided into sections and each section was modeled using the representation shown in Fig. 2. This model was preferred over a model with a single fuel lump coupled to a single graphite lump because of difficulties in defining appropriate average temperatures and outlet temperatures for a single fluid lump model.<sup>4</sup> If the outlet temperature of a single fluid lump model is assumed to be the same as the average temperature, then the steady-state outlet temperature is too low. If the average temperature is taken as a linear average of inlet temperature and outlet temperature, then it is possible for outlet temperature changes to have the wrong sign shortly after an inlet temperature

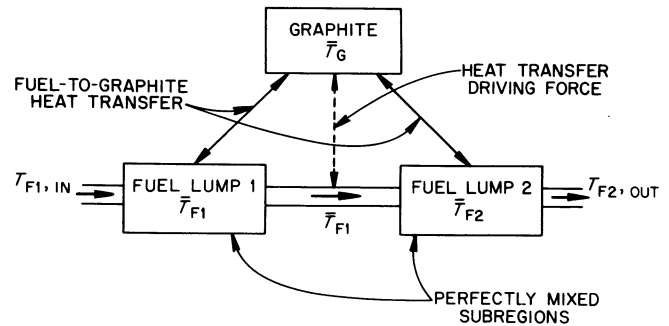


Fig. 2. Model of reactor core region; nuclear power produced in all three subregions.

change. The model using two fluid lumps circumvents these problems by providing an intermediate temperature to serve as an average temperature to use in the solid-to-liquid heat transfer calculations. Also, the average temperature in the second lump is a better representation of the outlet temperature than the average temperature of a single lump.

Since  $\sim 7\%$  of the heat is generated in the graphite by gamma ray and neutron interaction, the graphite lump equation has an internal heat source term. The equations are:

$$\begin{aligned} \frac{d\delta T_{f1}}{dt} = & \frac{K_{f1}}{(MC)_{f1}} \delta P + \frac{1}{\tau_{f1}} [\delta T_{f1}(\text{in}) - \delta T_{f1}] \\ & + \frac{(hA)_{f1}}{(MC)_{f1}} [\delta T_G - \delta T_{f1}] \end{aligned} \quad (6)$$

$$\begin{aligned} \frac{d\delta T_{f2}}{dt} = & \frac{K_{f2}}{(MC)_{f2}} \delta P + \frac{1}{\tau_{f2}} [\delta T_{f1} - \delta T_{f2}] \\ & + \frac{(hA)_{f2}}{(MC)_{f2}} [\delta T_G - \delta T_{f1}] \end{aligned} \quad (7)$$

$$\begin{aligned} \frac{d\delta T_G}{dt} = & \frac{K_G}{(MC)_G} \delta P - \left[ \frac{(hA)_{f1} + (hA)_{f2}}{(MC)_G} \right] \\ & \times [\delta T_G - \delta T_{f1}] \end{aligned} \quad (8)$$

where

$\tau$  = residence time

$h$  = heat transfer coefficient for a lump

$A$  = heat transfer area for a lump

$M$  = mass

$C$  = specific heat

$K$  = fraction of total power

$f_1$  = subscript indicating first fuel lump

$f_2$  = subscript indicating second fuel lump

$G$  = subscript indicating graphite.

In most of the calculations, 9 sections of the type shown in Fig. 2 were used giving a total of 27 lumps. The arrangement is shown in Fig. 3. The fraction of the total power generated in each lump was obtained from steady-state calculations of the power distribution. The local temperature coefficients were obtained for each region by importance weighting the computed overall temperature coefficients for fuel and for graphite.

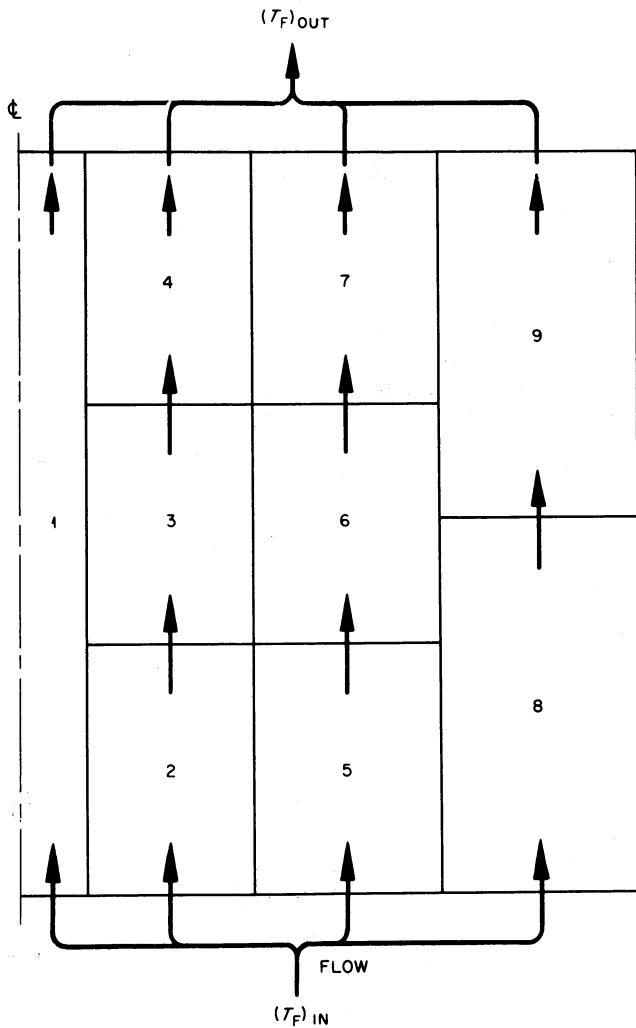


Fig. 3. Schematic diagram of 9-region core model.

**D. Heat Exchanger and Radiator**

The models for the heat exchanger and the radiator were similar to the core heat transfer models. The arrangement for a heat exchanger section appears in Fig. 4. The equations for a heat exchanger section are:

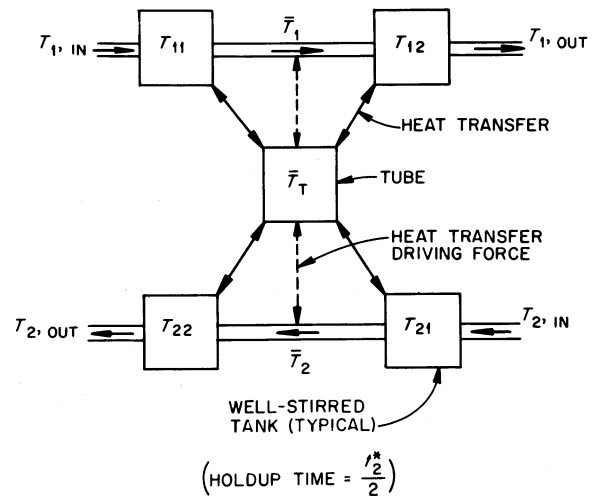


Fig. 4. Model of heat exchanger and radiator section.

$$\frac{d\delta T_{11}}{dt} = \frac{1}{\tau_{11}} [\delta T_{11}(\text{in}) - \delta T_{11}] + \frac{(hA)_{11}}{(MC)_{11}} [\delta T_T - \delta T_{11}] \quad (9)$$

$$\frac{d\delta T_{12}}{dt} = \frac{1}{\tau_{12}} [\delta T_{11} - \delta T_{12}] + \frac{(hA)_{12}}{(MC)_{12}} [\delta T_T - \delta T_{11}] \quad (10)$$

$$\frac{d\delta T_T}{dt} = \frac{(hA)_{11} + hA_{12}}{(MC)_T} [\delta T_{11} - \delta T_T] + \frac{(hA)_{21} + hA_{22}}{(MC)_T} [\delta T_{21} - \delta T_T] \quad (11)$$

$$\frac{d\delta T_{21}}{dt} = \frac{1}{\tau_{21}} [\delta T_{21}(\text{in}) - \delta T_{21}] + \frac{(hA)_{21}}{(MC)_{21}} [\delta T_T - \delta T_{21}] \quad (12)$$

$$\frac{d\delta T_{22}}{dt} = \frac{1}{\tau_{22}} [\delta T_{21} - \delta T_{22}] + \frac{(hA)_{22}}{(MC)_{22}} [\delta T_T - \delta T_{21}] \quad (13)$$

In some of the calculations, it was assumed that the heat capacity of the air in the radiator was negligible. (Terms  $T_{21}$  and  $T_{22}$  are used for the air side of the radiator.) Ignoring the heat storage in the air leads to the following heat balance:

$$(WC)_{21} [T_{22} - T_{21}(\text{in})] = (hA_{21} + hA_{22})(T_T - T_{21}) \quad (14)$$

where  $W$  is the mass flow rate of the air.

If we assume  $T_{21} = [T_{21}(\text{in}) + T_{22}]/2$ , Eq. (14) becomes

$$\frac{(WC)_{21}}{(hA_{21} + hA_{22})} [2T_{21} - 2T_{21}(\text{in})] = [T_T - T_{21}] \quad (15)$$

Now, we write the equation in terms of incremental quantities and assuming  $T_{21}$  (in) is constant to obtain:

$$\delta T_{21} = \frac{\delta T_T}{1 + 2 \frac{(WC)_{21}}{hA_{21} + hA_{22}}} \quad (16)$$

This is then used for  $\delta T_{21}$  in Eq. (11). The schematic representation of this type of radiator model appears in Fig. 5.

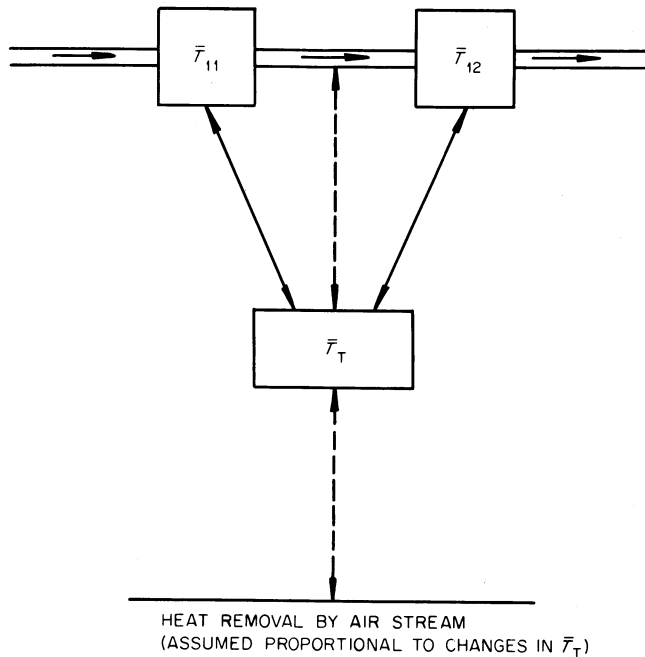


Fig. 5. Model of radiator for assumed negligible air heat capacity.

E. Piping

Several models were used to represent salt transport in the piping in different stages of the studies. The simplest model was a pure time delay. From some calculations (eigenvalues of the systems matrix) it was necessary to eliminate the delay terms. They were represented by Padé approximations<sup>5</sup> in those calculations. In some of the more detailed calculations, the heat transfer to the pipe walls was included. Since experimental results<sup>1</sup> obtained after the <sup>235</sup>U study indicated significant mixing in headers and piping in the fuel stream, some calculations for the <sup>235</sup>U fueled system used a model of a mixing chamber at the core outlet. This model consisted of the following equation (a first-order lag):

$$\frac{d\delta T}{dt} = \frac{1}{\tau} (\delta T_{in} - \delta T) \quad (17)$$

F. Values of Important Parameters

Some of the important parameters computed for the <sup>235</sup>U and <sup>233</sup>U loadings appear in Table I.

G. Overall System Model

The models for the subsystems were combined to give an overall system model. Several different overall system models were used in different stages of the study. The model shown in Fig. 6 was used in the study of the <sup>233</sup>U-fueled system. This will be called the reference model. This model resulted in a 44'th-order system matrix with 4 time delays for heat convection and 6 time delays for precursor circulation. Major modifications of this model which were used in some

TABLE I  
Parameters Used in MSRE Dynamics Studies

Parameter	<sup>235</sup> U	<sup>233</sup> U
Fuel reactivity coefficient (°F <sup>-1</sup> )	-4.84 × 10 <sup>-5</sup>	-6.13 × 10 <sup>-5</sup>
Graphite reactivity coefficient (°F <sup>-1</sup> )	-3.70 × 10 <sup>-5</sup>	-3.23 × 10 <sup>-5</sup>
Neutron generation time (sec)	2.4 × 10 <sup>-4</sup>	4.0 × 10 <sup>-4</sup>
Total effective delayed-neutron fraction (fuel stationary)	0.00666	0.0029
Total effective delayed-neutron fraction (fuel circulating)	0.00362	0.0019
Total fuel heat capacity (in core) (MW sec/°F)		4.19
Heat transfer coefficient from fuel to graphite (MW/°F)		0.02
Fraction of power generated in the fuel		0.934
Delayed power fraction		0.0564
Core transit time (sec)		8.46
Graphite heat capacity (MW sec/°F)		3.58
Fuel transit time in external primary circuit		16.73
Total secondary loop transit time (sec)		21.48

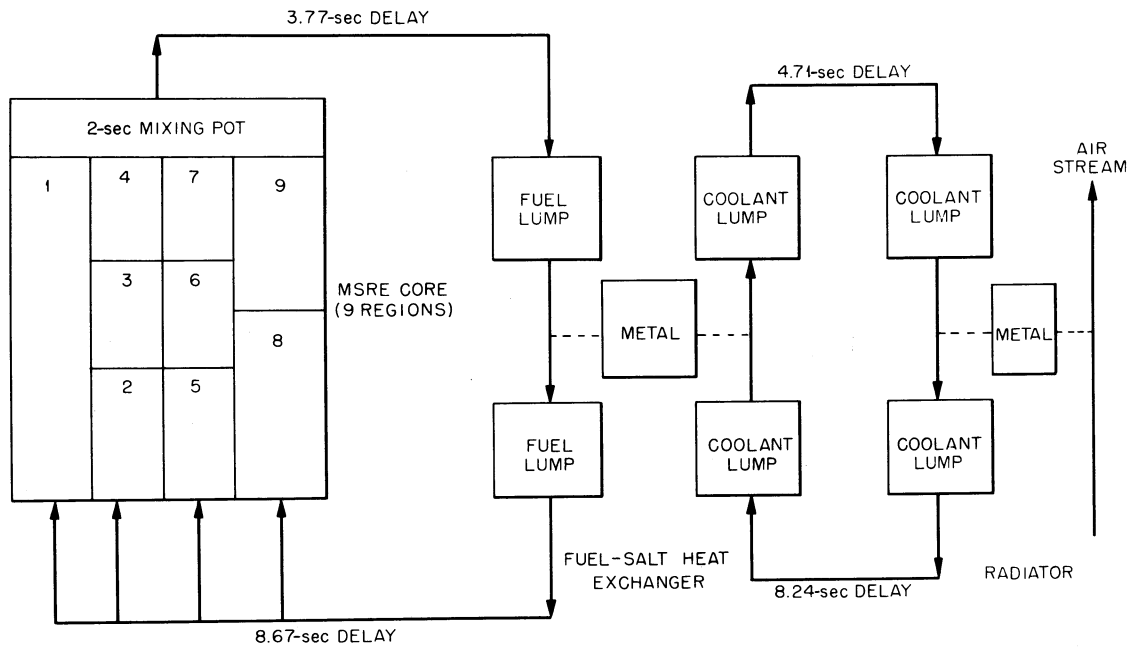


Fig. 6. Schematic representation of the MSRE reference model.

aspects of the study are listed below:

1. The mixing pot was not included in the early studies for the <sup>235</sup>U-fueled systems. It was added after experimental results<sup>1</sup> indicated significant mixing of the fuel salt.

2. For computing the eigenvalues of the system matrix, each pure time delay for fluid transport was replaced by a Padé approximation. Effective delayed-neutron fractions were determined and Eq. (3) was used instead of Eq. (2).

3. In the models used in the MSFR code (see Sec. IV), the heat exchanger and radiator models were expanded. Instead of a single 5-node representation for the heat exchanger, 10 sections (each with 5 nodes) were used. Instead of a single 3-node representation for the radiator, 10 sections (each with 3 nodes) were used as with the heat exchanger.

Calculations showed that results obtained with the simpler heat exchanger and radiator models gave good agreement with results obtained using the larger models for these components.

#### IV. METHODS OF ANALYSIS

##### A. Transient Response

The transient response of the reactor system was calculated for selected input disturbances

(usually reactivity steps). The computer code MATEXP<sup>6</sup> (a FORTRAN IV program for the IBM-7090 or IBM-360) was used for these calculations. MATEXP uses the matrix exponential technique to solve the general matrix differential equation. For the linear case, the general matrix differential equation has the form:

$$\frac{d\bar{x}}{dt} = A\bar{x} + \bar{f}(t) \quad (18)$$

where

$\bar{x}$  = the solution vector

$t$  = time

$A$  = system matrix (a constant square matrix with real coefficients)

$\bar{f}(t)$  = forcing function vector.

The solution of Eq. (18) is

$$\bar{x} = \exp(At)\bar{x}(0) + \int_0^t \exp[A(t - \tau)]\bar{f}(\tau)d\tau \quad (19)$$

MATEXP solves this equation using a power series for the evaluation of  $\exp(At)$ :

$$\exp(At) = I + (At) + \frac{1}{2}(At)^2 + \dots \quad (20)$$

In MATEXP,  $f(\tau)$  must be a step or representable by a staircase approximation. For the nonlinear case, the general matrix differential equation is

$$\frac{d\bar{x}}{dt} = A\bar{x} + \Delta A(\bar{x})\bar{x} + \bar{f}(t) \quad (21)$$